Bullion production in imperial China and its significance for sulphide ore smelting world-wide

CrossMark

Siran Liu [a, *], Thilo Rehren [b], Jianli Chen [c], Changqing Xu [d], Pira Venunan [a], David Larreina-Garcia [a], Marcos Martinón-Torres [a]

[a] UCL Institute of Archaeology, London, UK
[b] UCL Qatar, Doha, Qatar
[c] School of Archaeology and Museology, Peking University, Beijing, China
[d] Jiangxi Provincial Institute of Archaeology, Nanchang, China

ARTICLE INFO

ABSTRACT

Gold and silver production was of major importance for almost all ancient societies but has been rarely studied archaeologically. Here we present a reconstruction of a previously undocumented technology used to recover gold, silver and lead at the site of Baojia in Jiangxi province, China dated between the 7th and 13th centuries AD. Smelting a mixture of sulphidic and gossan ores in a relatively low temperature furnace under mildly reducing conditions, the process involved the use of metallic iron to reduce lead sulphide to lead metal, which acted as the collector of the precious metals. An experimental reconstruction provides essential information, demonstrating both the significant influence of sulphur on the silicate slag system, and that iron reduction smelting of lead can be carried out at a relatively low temperature. These new findings are relevant for further studies of lead and precious metal smelting slags world-wide. The technological choices of ancient smelters at this site are then discussed in their specific geographical and social-economic settings.

1. Introduction

In China gold and silver became prestige metals later than in other regions of the world (Bunker, 1993, 1994), but since the Tang and Song Dynasties (7th–13th century), after these metals were culturally accepted as symbol of wealth and social status, they were widely used for gift giving, wealth stock, trade, tax paying and item production (Katō, 2006 [1926]; Qi, 1999; Gyllensvard, 1957). Archaeologically, ancient gold and silver mines and large heaps of relevant production remains have been identified in many different regions of China. Nonetheless, our knowledge about the early production of gold and silver is limited and a handful of publications (e.g., Yi, 1972; Xie and Rehren, 2009; Zhou et al., 2014) can only portray a fragmented picture. Here, we present analytical results from the gold and silver production site of Baojia in Jiangxi province, central-south China, which is expected to set a framework for future studies of precious metals production in ancient

China. Since the technology indicated by smelting remains from this site is quite unusual (see Discussion), a series of question-based pilot experiments were conducted to test our reconstruction.

2. Background

2.1. Archaeological background

Baojia is located in the eastern part of Jiangxi province. During the imperial period, it was part of the *Xin Zhou* state (Fig. 1). The historical gazetteer of *Xin Zhou* recorded that mining of gold in Baojia started in the era of *Xuanhe* (AD 1119–1125) and finished shortly after, in the third year of *Jianyan* (AD 1129) (see Wang, 2005, 19). Since 2009, a joint investigation of this site has been conducted by Peking University and Jiangxi Provincial Institute of Archaeology. Remains of ancient metal production including slag, furnace fragments, beneficiation facilities, mining galleries and the residential area of workers have been identified. The smelting district was found in a small valley close to the mining district (Fig. 2). Five shovel tests were conducted in different parts of the district in order to gauge the area and depth of smelting remains. Slags,
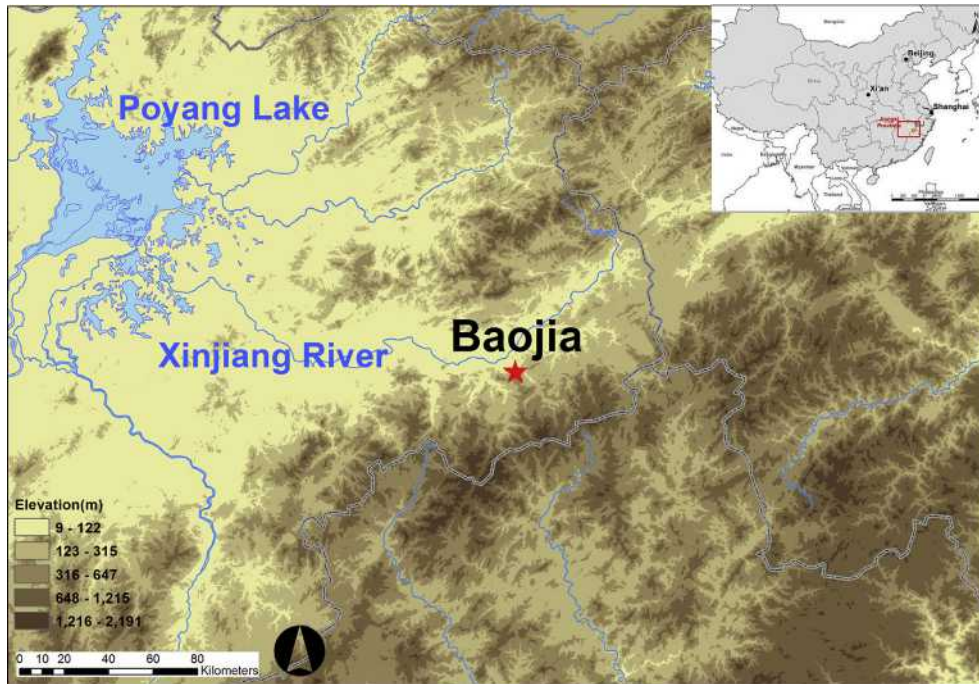
Fig. 1. Map showing the site of Baojia in the eastern part of Jiangxi province, connected to the lake Poyang by the Xinjiang River (as in the figure).

furnace fragments and pottery sherds were recovered from under a layer of agricultural soil, but matte (metal sulphide) was not found in any of these tests. The layer containing smelting remains is between 30 and 70 cm thick with the thickest part close to modern buildings (Fig. 3). The slag-bearing area was estimated to be around 8000 m² , based on surface survey and shovel tests, and indicates small to medium scale production. Standing smelting installations or furnace base have not been identified at this site. All the currently recovered remains are identified to be associated with primary smelting process, presumably producing precious metal-bearing lead bullion (see also Discussion part). Remains of

cupellation, e.g. cupellation hearth and litharge, have not been identified and therefore it is hard to tell whether separation between lead and precious metal was conducted in the same area. A more detailed description of metallurgical remains of this site and its chronology will be published in a forthcoming survey report in Chinese.

2.2. Models of primary production of precious metals

Most gold and silver ores contain these precious metals only in a fraction of a percent, and are therefore hard to be smelted directly.

Fig. 2. Satellite image of the site of Baojia. The smelting district is approximately 2 km northwest of the mining district. The potential area of smelting remains is approximately 8000 m² .

Fig. 3. Smelting district at Baojia. It is covered by vegetation and the thickest part of the slag heap is beneath modern buildings. The right picture shows the profile of one test pit. Beneath the black layer of smelting remains is the original sandy soil.

Instead, they have to be smelted together with a more abundant base metal, usually lead, which has a strong affinity to them (Bachmann, 1995; Craddock, 1995, 221–228). Gold and silver are thus collected in a lead bullion, from which the precious metals can then be further extracted by cupellation and parting.

In pre-modern periods, there were three main ways to smelt gold/silver-bearing sulphidic lead ores (Kassianidou, 1992, 36–37). Roast-reduction produces lead from the reaction between lead oxide and lead sulphide in a mixed ore (Blanchard, 1992; Gill, 1992; Rosenqvist, 1983, 341). This technology can be done in simple furnaces while recovering most of the silver in lead, but requires large pieces of high quality ore (Bayley et al., 2008, 53) and the yield of lead can be low, around 60% (Blanchard, 1992). The second method is a two steps process called roasting-smelting (Kassianidou, 1993; Rosenqvist, 1983, 267–268). Roasting is

conducted in the same low temperature range as the co-smelting process, but in a more open structure with a more oxidising atmosphere (Marechal, 1985). The roasted ore will then be charged into a smelting furnace for lead extraction. The third method, here called Iron Reduction Process (IRP), used iron scraps instead of carbon as the reducing agent in the smelting installations (Rosenqvist, 1983, 342; Percy, 1870, 219). Iron has a high affinity for sulphur and is able to reduce metals such as lead from their sulphides (Figure 10 in Rehren et al., 2012). The pre-modern use of this technology is only documented by a few historical sources (Dube, 2006; Institute of Qing History and Department of Archives, RUC, 1983, 383; Zhou et al., 2014) and, to our knowledge, it had rarely been studied archaeologically prior to the current project (Zhou et al., 2014). The benefit of this method is that roasting is not necessary while all types of lead compounds (both oxides and
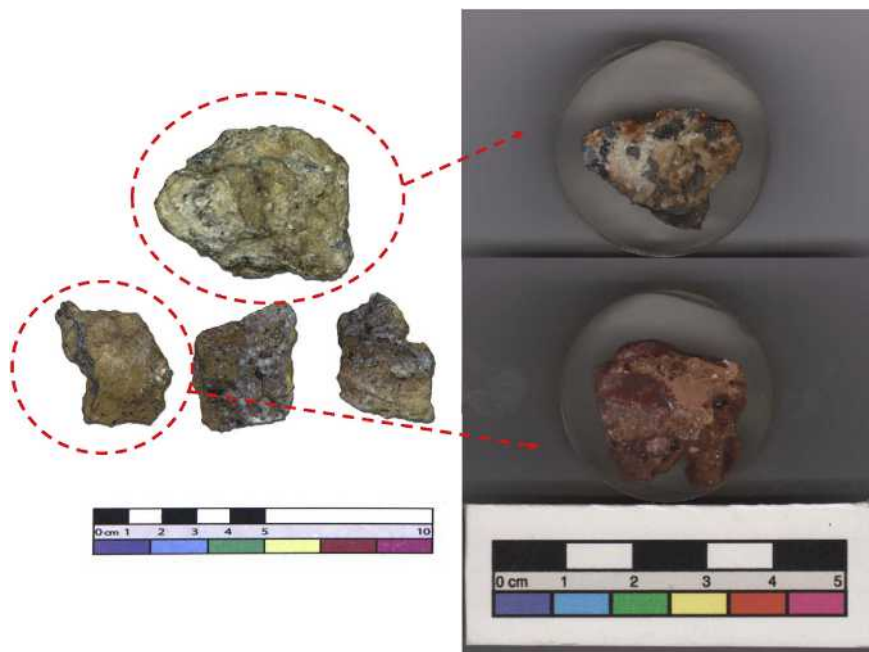

Fig. 4. Ore samples from the site of Baojia. The top sample is the primary sulphidic ore with grey coloured sulphide crystals. The three brownish pieces in the lower row are secondary gossan ores, identified by modern miners as gold ore. Macroscopically, they mainly consist of reddish iron oxide/hydroxide and quartz grains, and no visible metallic particles. (For interpretation of the references to colour in this figure legend, the reader is referred to the web version of this article.)

Table 1
^{14}C age in years before present (BP). The calibrated age in calendar year was given in ± 2σ. All dating work was done at the Peking University Radiocarbon Dating Laboratory.

Code	PKU Lab code	^{14}C age ± 1σ year BP	Calibrated age with ± 2σ AD	Context
BJG-C1	BA130871	845 ± 25	1158–1256	Profile of testing pit
BJG-C2	BA130872	1350 ± 25	640–763	Profile of testing pit
BJG-C3	BA130873	1305 ± 25	660–768	Profile of testing pit
BJG-C4	BA130874	880 ± 25	1045–1220	From metallurgical deposit
BJG-C5	BA130875	1030 ± 25	973–1032	From metallurgical deposit
BJG-C6	BA130876	1085 ± 25	895–1015	From metallurgical deposit
BJG-C7	BA130877	1125 ± 30	777–991	From metallurgical deposit
BJG-C8	BA130878	800 ± 20	1211–1270	From metallurgical deposit

sulphides) can be reduced. Consequently, the loss of lead and precious metals in this process can be avoided, and much less residual lead will be left in smelting remains.

3. Samples

Geological ore samples were acquired from ancient and modern mines near Baojia (see Fig. 2), including the sulphidic primary ores and quartz-rich gossan ores. Primary galena-rich ore was collected from an ancient mining gallery, and gossan ore was provided by current gold miners at the site, who leach the ore with cyanide to extract gold. Macroscopically, the gossan ore is rich in quartz and covered by red-orange rust (Fig. 4).

Charcoal samples for radiocarbon dating were collected from the profile of one shovel test pit and from the soil dug out from the layer of smelting remains (Fig. 3). Radiocarbon dating (Table 1) places the site between the 7th and 13th century AD (from the Tang to the late Song and the early Yuan dynasty), in agreement with historical documents. More detailed discussion about chronology

and methodology of radiocarbon dating will be presented in the survey report in Chinese.

Since these charcoal samples were all recovered from shovel tests, the dating results should only be considered as preliminary. Accordingly, the emphasis of this paper is on the technological reconstruction and its interpretation within a relatively broad historical setting.

Thirty-two slag samples were selected for chemical and mineralogical analyses, with 5–10 samples from each shovel test pit. All slags are dense and black. Flow patterns were observed on the upper surface of most samples whereas in the lower side, many small sand grains were found (Fig. 5), characterising these as tap slags.

4. Analytical methodology

All archaeological and experimental samples were mounted as polished blocks following standard procedure for optical microscopy. The blocks were then carbon coated and examined with a JEOL JXA8600 microprobe. An Oxford Instruments X-sight Energy Dispersive Spectrometer (EDS) and INCA analytical software package were used to collect and process compositional data. The excitation voltage was set as 20 kV and the beam current at 50 nA for a working distance of 11 mm. A cobalt standard was used to monitor the stability of beam current and peak identification. Bulk compositions of slag and matte inclusions were determined by averaging 3–5 area analyses of 1 mm by 0.8 mm each. USGS BHVO-2 basalt, NIST 1412 glass and Corning B glass were used as reference materials to monitor the EDS data quality (Table 2). For all relevant elements when their concentrations are above 0.5wt%, the analytical result of EPMA-EDS has an error margin around or lower than 10%. When the absolute concentrations are between 0.1wt% and 0.5wt%, the analytical result is much less reliable.

Fig. 5. Slag samples collected from the site of Baojia. Six fragments were selected from the Baojia slag samples, most of which look quite similar to each other. Flow pattern on their surface and sand inclusions on the underside indicate they were tapped from a furnace.

Table 2
Published values and measured results for three standard materials (USGS BHVO-2 basalt, NIST 1412 glass and Corning B glass). All results are normalised and presented in weight percent. Raw analytical data of standards can be found in OSM (Online Supplementary Material). bdl = below detection limit. All three standards still have some other trace elements but since their concentrations are too low to be detected by EDS analysis, they are not listed here.

		Na$_2$O	MgO	Al$_2$O$_3$	SiO$_2$	P$_2$O$_5$	SO$_3$	K$_2$O	CaO	TiO$_2$	MnO	FeO	CuO	ZnO	SrO	CdO	BaO	PbO	Cl
USGS BHVO-2	Recommended value	2.24	7.30	13.64	50.40	0.27	–	0.53	11.51	2.76	0.17	11.18	–	–	–	–	–	–	–
	Mean (n = 6)	2.2	7.1	13.1	50.9	0.3	–	0.5	11.6	3.0	bdl	11.2	–	–	–	–	–	–	–
	Relative error %	1.8	2.7	3.9	1.0	11	–	5.7	0.78	8.7	–	0.18	–	–	–	–	–	–	–
NIST 1412	Recommended value	5.18	5.18	8.31	46.85	–	–	4.58	5.01	–	–	0.03	–	4.95	5.03	4.84	5.16	4.86	–
	Mean (n = 9)	5.8	5.0	7.9	46.8	–	–	4.5	5.0	–	–	bdl	–	5.0	5.0	5.0	5.2	5.1	–
	Relative error %	12	3.5	4.9	0.11	–	–	1.7	0.20	–	–	–	–	1.0	0.60	3.3	0.78	4.9	–
Corning B	Recommended value	16.90	1.02	4.33	61.19	0.82	0.54	0.99	8.51	0.88	0.25	0.30	2.64	0.19	0.02	–	0.12	0.61	0.2
	Mean (n = 8)	17.1	1.0	3.9	62.5	0.8	0.6	1.1	8.9	bdl	0.2	0.3	3.0	bdl	bdl	–	bdl	0.4	0.2
	Relative error %	1.2	2.0	9.9	2.1	2.4	11	11	4.6	–	20	0.0	14	–	–	–	–	34	0.0

5. Analytical results

5.1. Ore samples

BJG-Ore1 is a sulphidic ore mainly composed of arsenopyrite (FeAsS), galena (PbS), sphalerite (ZnS), pyrite (FeS$_2$), and quartz-rich gangue. Within galena crystals, small inclusions of complex silver sulfosalts (A$_m$B$_n$S) were identified containing considerable amounts of antimony and up to 69% silver (Table 3). BJG-Ore2 and BJG-Ore3 are both from the gossan and predominantly composed of a quartz matrix and clusters of haematite (Fe$_2$O$_3$). BJG-Ore3 is also dominated by quartz but has small sulfosalt, argentite (Ag$_2$S) and electrum (natural alloy of Au and Ag) particles with up to 40% gold. Based on these analyses, the gossan ores are thought to be the main source of gold, while primary ores contribute lead. Silver is present in both types of ores. The electrum particles in gossan ores are typically less than 10 μm in diameter and tightly embedded in a dense quartz matrix (Fig. 6). Physically separating these particles from the gangue through crushing and washing would carry a high risk of losing gold in the waste material. Using pyro-technology to melt the 'silica cage' of these particles reduces this risk (Bachmann, 1995).

5.2. Slag samples

The texture of Baojia slags is glassy but contains numerous sulphidic and metallic inclusions, as described below. The variation of chemical composition between samples is small and therefore, only means and standard deviations of each oxide components are reported in Table 4 while complete bulk chemical compositions of all 32 samples can be found in OSM.

Table 3
Chemical composition of gold and silver-bearing phases in Baojia ores, in weight percent. EPMA-EDS analyses, all result normalised to 100 wt%. bdl = below detection limit.

Code	Phase	Si	S	Fe	Cu	Zn	As	Ag	Sb	Au
BJG-ore1	Complex silver sulfosalt	bdl	23.3	2.3	25.0	4.7	bdl	17.0	27.7	bdl
BJG-ore1	Complex silver sulfosalt	bdl	23.6	2.5	24.9	3.9	bdl	16.5	28.6	bdl
BJG-ore1	Complex silver sulfosalt	bdl	16.9	4.8	12.3	1.4	3.1	46.7	15.0	bdl
BJG-ore1	Complex silver sulfosalt	bdl	15.6	bdl	3.8	bdl	bdl	67.0	9.4	4.4
BJG-ore3	Complex silver sulfosalt	bdl	17.1	bdl	0.9	bdl	1.4	67.3	13.2	bdl
BJG-ore3	Complex silver sulfosalt	0.5	16.6	bdl	1.1	bdl	1.5	68.4	11.9	bdl
BJG-ore3	Complex silver sulfosalt	1.2	18.0	bdl	1.3	bdl	bdl	65.2	14.3	bdl
BJG-ore3	Electrum	bdl	bdl	bdl	bdl	bdl	bdl	63.5	bdl	36.5
BJG-ore3	Electrum	bdl	11.5	bdl	bdl	bdl	bdl	56.3	bdl	32.3
BJG-ore3	Electrum	bdl	bdl	bdl	bdl	bdl	bdl	59.8	bdl	40.2
BJG-ore3	Electrum	bdl	bdl	bdl	bdl	bdl	bdl	62.4	bdl	37.6
BJG-ore3	Argentite	bdl	13.3	bdl	bdl	bdl	bdl	86.7	bdl	bdl

5.2.1. Slag matrix

The Baojia slags differ from typical early smelting slags (see Hauptmann, 2014, 99—100, also Hauptmann, 2007, 160—162 for copper smelting slags and Rehren et al., 2007 for iron smelting slags) by having slightly lower amounts of iron oxide than silica. In addition, they are sulphur-rich (approx. 3 wt% expressed as SO$_3$). Lead content of all slag samples is generally low and only slightly above 0.5 wt%. Their microstructure is quite peculiar. Instead of the typical lath-shaped or hopper olivine of fayalitic tap slags, the Baojia slag is predominantly glassy, although small granular phases can sometimes be observed (Fig. 7). The glassy matrix consists of an iron-rich bright phase and a silica-rich globular dark phase (Table 5, Fig. 7). A relatively minor grey-shade phase which is rich in lime can also sometimes be found.

5.2.2. Matte prills

Prills identified in Baojia slag are mainly metal sulphides (matte), commonly pyrrhotite (Fe$_{1-x}$S), cubanite (CuFe$_2$S$_3$), bornite (Cu$_5$FeS$_4$) solid solution (Fig. 8), and sometimes the intergrowth between PbS and a complex system of copper and iron sulphides (Cu—Fe—S) (Fig. 9). The abundance of matte inclusions in the samples suggests that a discrete matte layer may have formed beneath the slag. Only relatively large matte prills (>c.10 μm) were analysed (Table 6). Apart from the three major components (Fe, Cu, S), lead, antimony and silver are found abundantly in these prills.
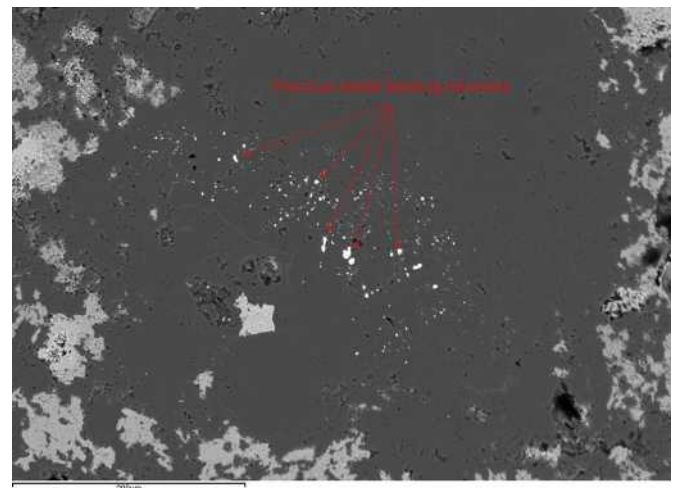

Fig. 6. BSE image of BJG-Ore3. Small bright particles in the middle of the picture are electrum and other precious metal-bearing minerals. They are firmly embedded in quartz (dark grey). The light grey phase is haematite. The very small particle size of precious metal-bearing minerals makes it hard to concentrate them mechanically.

Table 4
Bulk chemical composition of all 32 Baojia slags in weight percent, normalised to 100 wt%. Lead was found just above the detection limit of EDS (c. 0.5 wt%) in most of the bulk analyses.

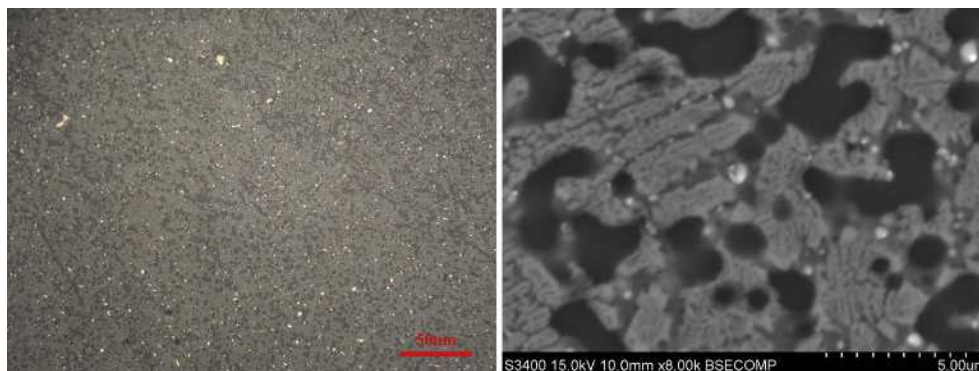|	MgO	Al_2O_3	SiO_2	P_2O_5	SO_3	K_2O	CaO	TiO_2	MnO	FeO	ZnO	PbO
Mean	0.5	4.3	44.8	0.1	2.9	2.0	3.2	0.4	1.7	39.0	0.3	0.8
Std.	*0.1*	*0.5*	*2.9*	*0.1*	*0.4*	*0.1*	*0.2*	*0.1*	*1.0*	*2.1*	*0.2*	*0.3*
Max.	0.6	5.7	49.9	0.3	3.6	2.3	3.9	0.6	4.3	42.3	0.8	1.6
Min.	0.2	3.7	39.7	0.0	2.0	1.8	2.8	0.0	0.9	34.9	0.1	0.4

Std. = Standard deviation.

Fig. 7. Plane polarized optical (left) and BSE (right) image of Baojia slag matrix. The slag has a glassy matrix and sometimes shows dark globular phases. High magnification BSE imaging shows a complex phase separation structure of bright, grey and dark phases.

The composition of these large prills varies considerably, and therefore can only give a range of composition that the potential matte cake should fall in. The raw data of matte prill analysis can be found in OSM. It is noted that the silver content of these particles is quite high with an average of 2.5 wt%, and suggests that a significant amount of silver was trapped in matte.

5.2.3. Speiss

Within the matte prills there are two frequent types of inclusions. The first is antimony speiss, mainly composed of Cu–Ni–Sb and Ag_3Sb. Arsenic was only found as a minor component in speiss from this site. Given that speiss is only partially miscible with matte, it might have formed a separate melt in the furnace (Rehren et al., 2012; Thornton et al., 2009; Rosenqvist, 1983, 343). Since large speiss particles are relatively rare and their composition varies significantly, all analytical results with their totals are presented in Table 7. Despite the variation of other elements, the silver content in these particles remains high with an average of 18.7 wt%, making it the main silver-bearing phase in matte.

5.2.4. Metallic iron

The second major inclusion in matte is metallic iron, occurring in two types—angular and rounded particles (Fig. 10). Typically, angular particles are deeply trapped inside large matte prills, while rounded iron particles usually contain numerous iron sulphide inclusions and have a thinner sulphide shell than those of the angular

particles. There is no clear pattern in the distribution of these two types of iron phases and in many cases, both of them were identified in the same slag sample. Different shapes of metallic iron in slag samples are usually explained by variation in smelting temperature and redox condition (Tholander, 1989; Killick and Gordon, 1989). More rounded prills are generally taken as indicative of furnaces operated at higher temperature and more reducing atmosphere. However, the formation mechanism of metallic iron in Baojia needs to be explained differently since rounded and angular particles were often found together. According to previous studies of the Cu–Fe–S system, metallic iron dissolves in the sulphides at temperatures above 1000 °C (Starykh et al., 2010). Upon cooling, metallic iron would first crystallise as cubic γ-Fe or α-Fe, enriching the rest of the melt in copper (Voisin and Itagaki, 2006) (Fig. 11).

However, iron created at high temperature and reducing atmosphere tends to be carburised immediately (Voisin and Itagaki, 2006) and then becomes molten and rounded. Therefore, only in those matte prills where the sulphide shells are thick enough to protect the iron from carburisation, angular iron particles were preserved. Otherwise, with increasing iron metal formation the iron particles would conglomerate, being carburised and becoming molten (Fig. 12). Occasionally wüstite and dendritic iron particles were also identified in matte prills (Figs. 8 and 13). It may indicate that some of the iron first crystallised as ferrous oxide and then was reduced inside the prills into its metallic state (see Discussion part).

Table 5
Chemical composition of three main phases in Baojia slag matrix in weight percent, normalised to 100 wt%.

Code	Phase	MgO	Al_2O_3	SiO_2	P_2O_5	SO_3	K_2O	CaO	TiO_2	MnO	FeO
BJG-slag-5-1	Black/globular phase	bdl	7.4	72.6	bdl	bdl	5.0	2.1	bdl	bdl	12.9
BJG-slag-5-1	Bright phase	0.9	2.5	43.8	bdl	0.8	2.1	1.1	bdl	1.3	47.5
BJG-slag-5-1	Grey glass	bdl	7.1	48.6	1.0	1.2	1.1	13.4	1.8	0.8	25.0

* It must be noted that due to the small size of individual black/globular phase and grey phase, their chemical composition acquired through SEM-EDS analysis may be analytically mixed by the volume of the electron beam.
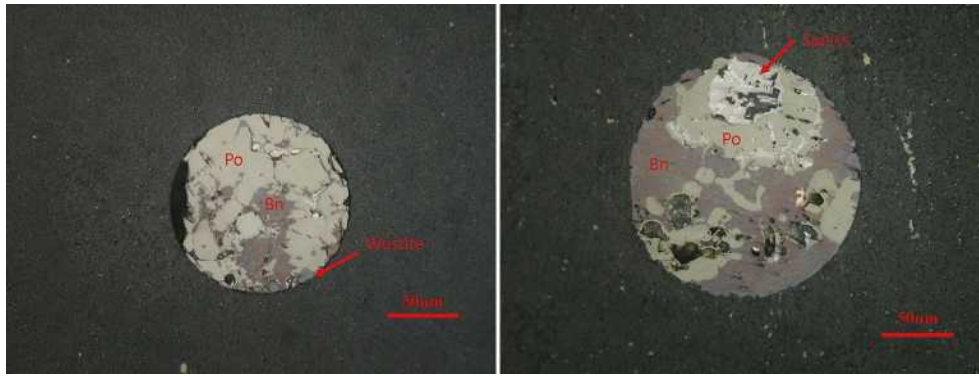
Fig. 8. Micrographs of two matte prills in Baojia slag. Both of them are dominated by pyrrhotite (Po) and bornite (Bn) solid solution. Speiss and wüstite particles were also identified in these particles.
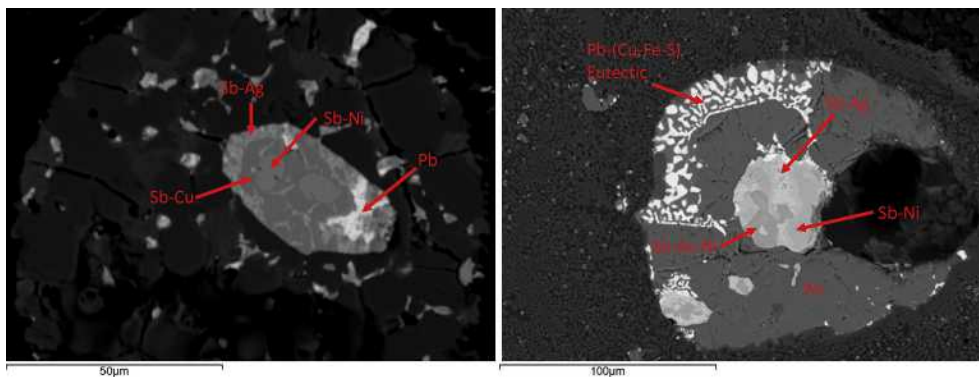

Fig. 9. Speiss present in Baojia matte inclusions, consisting of multiple phases.

5.2.5. Lead and silver

Occasionally, argentiferous lead and silver metal inclusions were identified in matte prills as well. The lead inclusions are small (less than 10 μm) and their composition may not be representative of the lead bullion produced. The bulk composition of these prills is quite variable but typically shows 2–3 wt% Ag, rarely reaching more than 50 wt%. Metallic silver was found associated with lead and speiss, and typically contains 2–20 wt% Sb. Gold was rarely identified, with a mere eight (in four different samples) out of more than four hundred EDS analyses revealing gold. Interestingly, in all cases, gold was found associated with metallic silver (Fig. 14) rather than with speiss or matte. This may reflect that gold has a stronger affinity to metallic silver and will preferentially partition with silver into metallic lead.

6. Experimental reconstruction (see OSM for experimental conditions and re-melting tests)

The results of our analyses of the slag samples indicated a considerable degree of interaction between silicate and sulphide melts, and the presence of metallic iron in the matte inclusions pointed to the potential use of the iron reduction process (IRP) at Baojia. Based on these observations, a series of experiments were conducted to test our reconstruction of the smelting process at Baojia, and to investigate the proposed reaction mechanism of lead

Table 6
Chemical composition of matte globules in Baojia slag samples in weight percent, normalised to 100 wt%. This is a summary of 82 bulk prill analyses, giving the range of composition for potential matte produced at this site.

	O	S	Fe	Ni	Cu	Zn	As	Ag	Sb	Pb
Mean	1.4	26.6	47.6	0.3	12.1	bdl	0.4	2.5	4.3	4.8
Std.	4.5	5.6	13.6	0.7	7.4	0.2	0.9	2.5	5.7	9.2
Max	22.2	36.5	77.9	2.7	39.0	1.2	6.6	14.4	32.6	50.6
Min	bdl	11.6	14.5	bdl	3.3	bdl	bdl	bdl	bdl	bdl

The high Ag content of these globules is shaded.

Table 7
Chemical composition of speiss inclusions in Baojia slag samples in weight percent.

Code	S	Fe	Ni	Cu	As	Ag	Sb	Pb	Total
BJG-2-1	bdl	3.9	5.2	13.7	1.4	28.7	51.2	bdl	104.2
BJG-2-1	bdl	11.1	bdl	6.2	bdl	22.3	47.1	13.4	100.2
BJG-2-1	bdl	1.6	6.3	32.3	0.7	7.7	49.9	5.0	103.3
BJG-2-2	bdl	1.4	4.3	34.9	bdl	2.1	17.6	39.7	100.0
BJG-2-2	bdl	3.8	2.1	28.0	bdl	25.0	34.2	6.7	100.0
BJG-2-3	bdl	0.7	1.2	21.2	bdl	38.3	34.7	7.3	103.3
BJG-2-3	0.7	3.1	bdl	37.4	bdl	17.1	41.9	4.8	105.1
BJG-3-1	bdl	6.9	8.6	2.0	bdl	17.7	70.8	0.0	106.0
BJG-3-3	1.8	3.2	7.1	16.3	1.3	5.6	58.0	13.3	106.5
BJG-3-3	bdl	5.8	6.0	25.7	4.9	10.8	46.9	bdl	100.1
BJG-3-4	bdl	7.5	9.5	38.9	5.9	1.2	38.0	bdl	101.1
BJG-3-4	bdl	5.4	9.0	41.8	3.6	0.8	40.0	bdl	100.7
BJG-3-4	bdl	2.7	8.9	14.2	1.7	9.1	41.9	25.3	103.6
BJG-3-6	0.7	5.3	2.0	48.3	0.7	4.2	40.0	4.0	105.2
BJG-3-6	3.5	6.9	2.3	50.6	bdl	3.1	38.1	0.0	104.5
BJG-3-6	4.1	22.2	bdl	11.3	13.0	37.4	12.1	8.8	108.9
BJG-3-6	0.7	3.9	0.5	59.1	0.0	4.4	32.9	1.0	102.7
BJG-4-1	bdl	6.1	4.6	0.0	3.9	31.6	54.2	0.0	100.4
BJG-4-1	bdl	3.6	bdl	7.6	0.0	55.1	22.4	16.8	105.5
BJG-4-2	bdl	2.3	22.8	0.0	8.8	24.4	43.0	0.0	101.2
BJG-5-6	bdl	1.6	0.7	30.2	bdl	31.1	32.2	8.7	104.5
BJG-5-6	bdl	1.0	0.8	35.0	bdl	20.1	39.2	6.8	102.9
BJG-5-6	bdl	1.6	0.7	30.2	bdl	31.1	32.2	8.7	104.5

The high Ag content of speiss inclusions is shaded.

smelting using metallic iron (Table 8). Sample BJG-slag-4-2 was randomly selected to represent the Baojia slag, and a wüstite (FeO)- and sulphide-free bloomery iron smelting slag from Austria was used to simulate a slag matrix based on self-fluxing iron-rich quartz gangue, prior to its interaction with the sulphidic ore. Commercially available galena (PbS), pyrite (FeS$_2$) and chalcopyrite (CuFeS$_2$) were mixed to resemble archaeological ores. Re-melting tests showed that at 1100 °C the BJG-slag-4-2 became liquid, while the fayalitic bloomery slag remained solid. Experimental temperature was accordingly set as 1100 °C. In the first two experiments, the bloomery slag was mixed with galena and iron metal to simulate IRP. SL2 contained additionally pyrite to explore its role in the IRP. SL3 to SL5 were a series of re-melting experiments to study the interaction between matte and slag more generally. In order to test whether the interaction of sulphides and silicate melts is restricted to the presence of highly reactive substances -such as lead sulphide and metallic iron-, we conducted these experiments using the same bloomery slag and chalcopyrite ore as the sole ingredients. The chemical composition of the sulphidic phase in chalcopyrite ore analysed with EPMA-EDS is presented in Table 10.

6.1. Analytical results of iron reduction process experiments (SL1 and SL2)

Fig. 15 shows the cross-section of experiments SL1–SL2; the bulk chemical compositions of slag and matte produced are displayed in Tables 9 and 10, respectively. SL1, formed from the reaction of bloomery slag, galena and metallic iron, solidified as a porous body of slag with a significant amount of matte and metallic lead trapped in it, a thin separate matte layer and a lead cake at the bottom (Fig. 15 and Fig. 16). SL2, from a charge of bloomery slag, galena, pyrite and metallic iron, solidified into a denser body of slag with perfectly separated matte and lead layers beneath it. Both slags are fayalitic with large amounts of sulphidic inclusions. The smelting introduced significant amounts of sulphur (3.5wt% and 4.1 wt% as SO$_3$) and lead (1.0 wt% and 3.2 wt% as PbO) to the slag, mostly as finely dispersed matte inclusions. It is important to note that the sulphide inclusions in the slag and matte cakes are predominantly iron sulphide, which indicates an extensive reaction between iron and galena. The dendritic metallic iron particles in SL1 matte are likely to be the re-crystallised unreacted iron (Fig. 17)
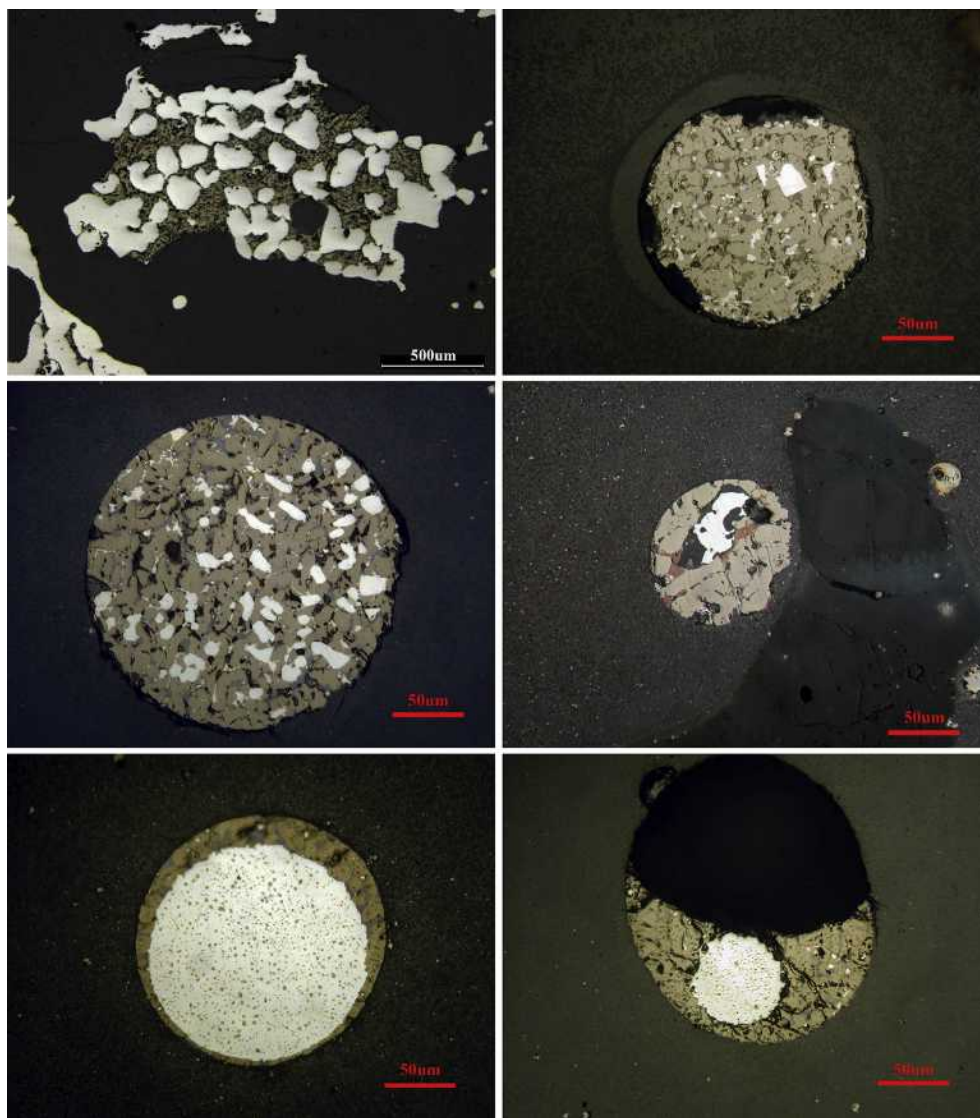

Fig. 10. Metallic iron prills and particles within matte globules in Baojia slag samples. The four images on the top show angular iron particles trapped in matte prills, while the two on the bottom show rounded iron particles with numerous sulphide inclusions. We see the angular and rounded iron particles as stages in a continuum of increasing metallic iron formation.
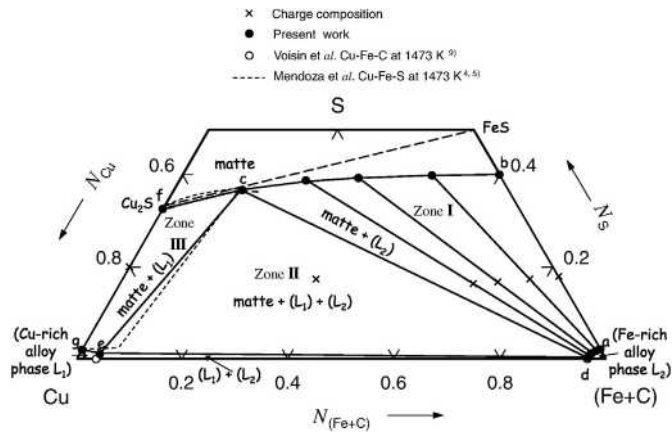
Fig. 11. Ternary diagram of the carbon-saturated Cu–Fe–S system at 1200 °C (1473 K) (in atom percent, after Voisin and Itagaki, 2006). Most matte prills bearing metallic iron particles fall in zone I. A melt in this zone (exemplified by four lines in the middle of this zone) will separate at this temperature into metallic iron (L_2, lower right corner) and a relatively copper-rich sulphide melt (top line of this zone, matte).

and indicate that the reaction in SL1 is less complete than SL2. The matte of experiment SL2 retained about twice as much lead (Table 10: 11 wt%) than the matte in SL1 (5.6 wt%), even though the charge for experiment SL2 contained additional pyrite while SL1 had only galena and metallic iron added to the bloomery slag. Furthermore, metallic lead prills and significant amounts of oxygen were identified in matte prills and cakes from both experiments. Apart from its increased lead and sulphur content and somewhat lower iron oxide, SL1 slag is not much different from the original bloomery slag. In contrast, SL2 slag has a significantly lower FeO/SiO_2 ratio than both the original slag and SL1, despite the fact that the SL2 charge was richer in iron than SL1, through the added pyrite.

6.2. The interaction of sulphides with silicate melts (SL3–SL5)

The slags from SL3–SL5 (bloomery slag with successive additions of chalcopyrite, Table 2) were all fully molten during the experiments, even though the pure bloomery slag would not melt at this temperature (see above). Through the repeated re-melting process, the FeO/SiO_2 ratio of the slag decreased significantly, though the experimental temperature remained the same and more iron was added to the batch with each addition of fresh chalcopyrite to the slag from the previous experiment (Table 8). The slags from SL4 and SL5 have similar chemical composition and phase separation structure to Baojia slag (Table 9, Fig. 18). This

structure seems to be associated with the silica-rich nature of these slags. The increased lime content of the slag is presumably due to calcium-bearing gangue present within the chalcopyrite ore. The composition of gangue minerals in chalcopyrite was not quantified in this research due to its limited relevance to the research aim; composition of chalcopyrite in Table 10 only reflects the average of the sulphide phases inside the ore. It is noticeable that the matte from all three experiments has a Fe/Cu weight ratio much higher than the original chalcopyrite (Table 10). Since no copper-rich phase was removed from the matte, this shift in ratio indicates the absorption of iron from the silicate melt into the sulphide melt.

7. Discussion

The discussion focuses on the reconstruction of the Baojia smelting technology in the light of experimental work. The interaction between silicate and sulphide melt will be further explored in a separate paper and is considered here only as far as it is relevant for the Baojia technology. Two observations in our experiments seemed counter-intuitive or demanded otherwise further exploration. First, the Baojia slag has a much lower melting temperature than the bloomery slag, even though it has considerably higher silica and lower iron oxide content. Second, there is a significant extent of ion exchange between silicate and sulphide melts, with a strong preference for iron to move from the slag into the matte.

7.1. Reconstruction of Baojia smelting technology

Dube (2006) suggested that lead smelting using the IRP would require a high operating temperature, since according to him only liquid iron could react effectively with lead sulphide. The presumed high operating temperature seemed reinforced when the composition of Baojia slag was plotted into the ternary FeO–Al_2O_3–SiO_2 system. In order to do this, the chemical composition was reduced to three main components (SiO_2–Al_2O_3–FeO) by adding MgO, CaO, MnO and ZnO to FeO (Fig. 19). Since the PbO content in all bulk analyses is very low, it is not likely to have had any considerable influence on the slag melting temperature. The melting temperature of Baojia slag suggested by this diagram is mostly between 1300 and 1500 °C, with a long 'tail' in the diagram crossing several isotherms, even though supposedly slag samples should follow the contour of the isotherms or fall within a trough between higher-melting compositions (Rehren et al., 2007). Furthermore, metallic iron was found within the Baojia samples co-existing with a silica-rich glassy slag, which is typically taken as indicative of furnaces operating not only at high temperature but also at strongly reducing conditions, as is required to prevent iron from entering
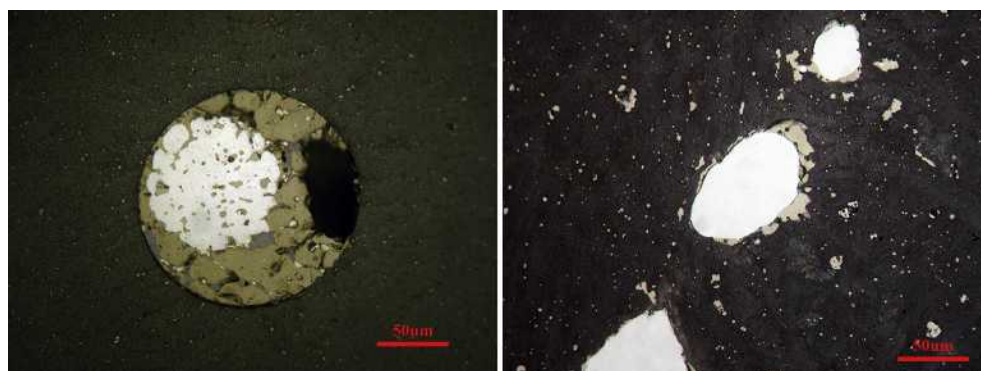

Fig. 12. Iron particles and prills in their transitional states. Left: iron particles begin to conglomerate. Right: iron particles become rounded into an irregular oval shape.

Fig. 13. Wüstite was occasionally identified within the matte prills (left). Dendritic iron particles (right).

slag as iron oxide (Fig. 3 in Freestone et al., 1985). Considering the relative ease of lead smelting (Tylecote and Merkel, 1985), it would seem hard to explain why such extreme conditions should have been employed in Baojia, especially when this was identified as a small scale production site which was only sparsely documented by the historical literature.

The re-melting experiment, however, demonstrated that the Baojia slag could be fully molten at 1100 °C (see OSM), which is in stark contradiction to the theoretical estimations. It is unlikely that the reduction of the multi-elemental slag composition into a three-component system is responsible for such a strong discrepancy; the three minor oxides that were added to the main oxides add up only to 5–6 wt% in total. Instead, we focus on the significant effect that a high sulphur content has on the melting behaviour of the slag.

1) In most studies of ancient smelting slags, the interaction of sulphides with the silicate slag is not considered. However, modern metallurgical and geological research shows that iron-rich sulphides interact with silicate melts (Fincham and Richardson, 1954; Yazawa, 1956; Maclean, 1969; Baker and Moretti, 2011 and references therein). Sulphur ions can enter the FeO-rich silicate melt through the following reaction (Poulson and Ohmoto, 1990).
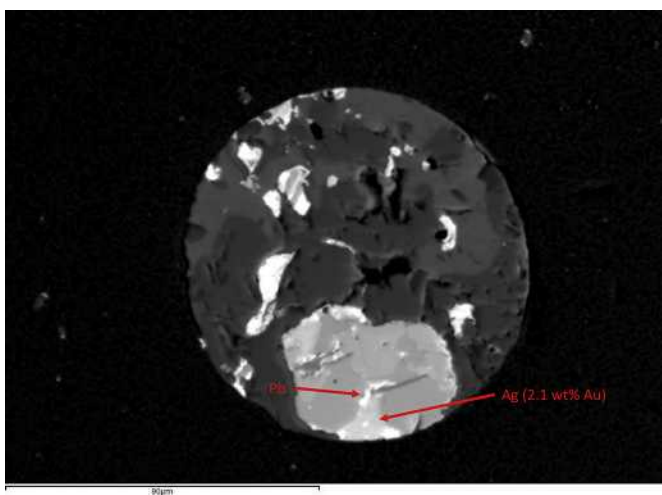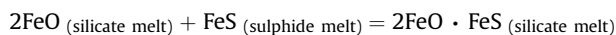
$$2FeO_{\text{(silicate melt)}} + FeS_{\text{(sulphide melt)}} = 2FeO \cdot FeS_{\text{(silicate melt)}}$$

Fig. 14. Gold containing speiss inclusion in BJG-slag-3-3. SEM-EDS analysis shows that the metallic silver phase trapped in the speiss contains 2.1 wt% Au. No gold was found in either the lead phase associated with silver or the speiss and matte surrounding them.

Sulphur ions can generally bring down the melting temperature of the silicate system (Maclean, 1969). Adding alumina or lime (6–7 wt%) to the sulphur-containing slag system will allow it to include significantly more silica at the same temperature (Yazawa and Kameda, 1953, 54 Table 3). At the same time, significant amounts of iron oxide can migrate into the sulphidic melt (Kaiura and Toguri, 1979; Fonseca et al., 2008). In our experiments, bloomery slag with an original liquidus temperature higher than 1100 °C became fully molten with various types of sulphide added, demonstrating the fluxing effect of sulphur in the iron oxide-silica system. It thus appears that the Baojia furnace could have operated at a relatively low temperature, despite producing a silica-rich glassy slag. The change in composition of the sulphide phase from the original ore minerals to the more iron-rich matte in the experiments SL3–SL5 demonstrates the chemical interaction of the two melt systems might have also happened in the archaeological case.

2) The widely distributed metallic iron particles and prills in the Baojia slags indicate that the ancient smelters used the IRP to produce lead bullion. It is unclear, however, whether the smelters added metallic iron as the active reagent, or whether the iron metal was formed *in situ* as part of the smelting process. Most of the iron particles found in the Baojia slag crystallised from the matte, making it difficult to suggest whether metallic iron was added to the furnace charge and dissolved in the matte, or was reduced *in situ*. Fig. 3 in Freestone et al. (1985) shows that reducing metallic iron from a silica-rich melt is harder than from free iron oxide, and requires a more reducing furnace. However, little previous research has considered the influence of sulphur in this process. As described above and observation in Fig. 13, liquid

Table 8
Crucible charges of four experiments.

Code	Charge	Aim
SL1	Bloomery slag 180 g; Galena 70 g; Iron 17 g	To explore the iron reduction process
SL2	Bloomery slag 180 g; Galena 70 g; Pyrite 30 g; Iron 17 g	To test the role of pyrite
SL3	Bloomery slag 180 g; Chalcopyrite 100 g	To study interaction between silicate slag and sulphidic ore more generally.
SL4	Slag from SL3 120 g; Fresh chalcopyrite 100 g	
SL5	Slag from SL4 120 g; Fresh chalcopyrite 100 g	

Table 9
Bulk composition of original and experimental slags in weight percent, normalised to 100 wt%. Large metallic and sulphide inclusions in these slags were excluded from the analyses.

Code	Descriptions	Al_2O_3	SiO_2	SO_3	K_2O	CaO	TiO_2	MnO	FeO	ZnO	CuO	PbO	FeO/SiO_2
Bloomery slag	−	5.3	32.3	bdl	0.7	bdl	bdl	3.0	58.7	bdl	bdl	bdl	1.8
SL1 slag	PbS + Fe	5.2	30.1	3.5	0.7	0.5	bdl	2.8	55.6	0.6	bdl	1.0	1.8
SL2 slag	PbS + FeS_2 + Fe	5.3	32.6	4.1	0.7	0.7	0.4	2.7	50.1	0.2	bdl	3.2	1.5
Bloomery slag	−	5.3	32.3	bdl	0.7	bdl	bdl	3.0	58.7	bdl	bdl	bdl	1.8
SL3 slag	Bloomery slag + $CuFeS_2$	6.2	33.0	2.6	0.8	0.5	bdl	2.8	53.0	1.0	bdl	bdl	1.6
SL4 slag	SL3 slag + $CuFeS_2$	5.7	40.0	3.7	0.7	3.1	0.4	2.8	41.9	1.7	bdl	bdl	1.0
SL5 slag	SL4 slag + $CuFeS_2$	7.1	44.1	3.3	0.7	5.0	0.0	2.7	37.1	bdl	bdl	bdl	0.8
Baojia slag average	−	4.4	45.1	2.9	2.0	3.2	0.4	1.8	39.4	bdl	bdl	bdl	0.9

Table 10
Bulk composition of matte produced during the experiments SL1—SL5 in weight percent, normalized to 100 wt%.

Code	Additives	O	S	Mn	Fe	Cu	Zn	Pb	Fe/Cu
SL1	PbS and Fe	3.3	28.9	bdl	62.3	bdl	bdl	5.6	−
SL2	PbS, FeS_2 and Fe	6.0	27.1	0.4	55.5	bdl	bdl	11.0	−
Chalcopyrite		bdl	36.9	bdl	31.9	34.7	bdl	bdl	0.9
SL3	Chalcopyrite	4.1	27.8	0.5	43.9	22.2	1.6	bdl	2.0
SL4	Chalcopyrite	3.5	28.7	0.5	40.9	23.6	2.8	bdl	1.7
SL5	Chalcopyrite	2.6	29.3	0.4	38.5	26.2	2.9	bdl	1.5

matte can dissolve large amounts of ferrous oxide which can then be reduced to metallic iron. The authors are currently unaware of any thermodynamic calculation of the relevant processes in an archaeological context, but the empirical evidence from the experiments reported above indicates the potential to separate iron oxide from a silicate structure and reduce it to metallic iron by means of this process, even without strongly reducing conditions.

Though it is difficult to differentiate iron reduced *in situ* from added metallic iron, we argue that for any of these mechanisms, lead smelting by IRP can be done at a relatively low temperature and mildly reducing conditions. Iron sulphides play an important role in this process since they can bring down the melting temperature of the slag, lead sulphide and metallic iron (Sharma and Chang, 1979; Erick and Ozok, 1994). Moreover, the sulphides presumably prevent the iron metal from (re-)oxidising by dissolving it in the sulphidic melt. Experiment SL1 and SL2 showed that without adding extra iron sulphide to the charge,

the reaction is slower and the separation between slag and metal is less perfect. However, it must be taken into account that the real smelting operated on a much larger scale and much longer time than in our experiments, and consequently the iron sulphide created in the smelting process would probably eventually gather to a significant volume, providing a proper reaction environment.

7.2. Contextualised interpretation of Baojia technology and its archaeological implications

Based on the previous technical discussion, the Baojia technology can be summarised as one that used metallic iron (either added or reduced from the furnace charge) to reduce lead from its sulphide. The particular conditions in the furnace facilitated the breakdown of the auriferous quartz grains seen in the gossan ore, releasing the electrum into the melt. The free metallic lead then collected the gold and silver before forming a separate melt at the bottom of the furnace. The furnace temperature for this process was probably low (not necessarily much higher than 1100 °C) and the atmosphere only mildly reducing, while the sulphide content of the system ensured complete fusion of the quartz and hence full recovery of gold particles, even at this low temperature. Gold was rarely identified within the Baojia slag. However, considering its low concentration in the ores and our limited data and the analytical methods used, it is impossible at this stage of our research to estimate gold recovery efficiency.

Considering the sulphur content in the Baojia slag, a significant amount of matte might have been produced. The matte prills in the slag are high in silver (2—3 wt%, Table 6) and relatively low in lead.

Fig. 15. Cross-sections of SL1 (left) and SL2 (right). The material inside the crucible separated into three layers. Top: slag, middle: matte, bottom: lead.

Fig. 16. Cross-section of SL1 slag. Numerous metallic lead and matte prills were found trapped in the slag.

Most of the silver was trapped in antimony speiss phases within the matte. There is an ongoing debate in the European context whether argentiferous speiss produced as the by-product of smelting could be further desilvered (Craddock et al., 1985; Kassianidou, 1998). The high silver content of the matte from Baojia, reaching several percent by weight, certainly suggests that it should have been further processed, especially considering the cut-off grade for economic desilvering of lead metal in ancient times, estimated at around 500—1000 ppm (Tylecote, 1987, 140; Rehren and Prange, 1998). The Baojia smelters might have strived to increase silver recovery by further processing their matte and speiss, for instance by roasting and charging it back to the smelting furnace, since we have not yet found any matte cake in this site. However, as Kassianidou (1998) pointed out, speiss is a difficult material to work

and is even considered to be problematic by modern metallurgists (Bachmann 1982, 29; Rosenqvist, 1983, 343), and therefore desilvering speiss may not have brought much additional profit for ancient smelters. In general, the Baojia technology appears as not very efficient in terms of recovering silver.

An arguably more efficient method to improve silver recovery would have been to increase the lead/silver ratio in the furnace by adding more metallic lead or lead sulphide ores. Considering the relatively low lead content in both Baojia slag and matte prills, as well as the amount of free metallic iron, Baojia smelters would have been able to reduce more lead in the furnace by adding extra galena; the produced lead would have probably collected more silver from the system. There were several significant silver and lead mines located quite close to the site of Baojia (Zhang, 1954, 21—41; Golas, 1999, 106—136; Wang, 2005, 428—457; Katō, 2006 [1926], 391—434 for literature evidence). For example, there was one site called *Yan Shan* (铅山), which in Chinese means the mountain of lead; the literature of Tang, Song, and Yuan periods (7th—14th century) recorded it as a lead production site (Zhang, 1954, 25—34). It is geographically close to the site of Baojia, and the two sites are connected by the Xin River. If Baojia smelters had aimed to recover all the silver from their ore, it would not have been hard for them to import some lead from those adjacent areas. However, as we have seen in many cases, ore efficiency or metal yield was not the only concern of ancient smelters (Cohen et al., 2009; Shennan, 1999; Rehder, 1994). Production in Baojia most likely was a local activity and a relatively simple technology, and not embedded in a wider network as would have been necessary to import lead ores. Wang (2005, 175—206) has reviewed the taxation methods of the metal industries during the Song Dynasty and suggested several organisation methods of metal production for this period. In many cases, workers at small mines were only part-time and would still need to pay their main tax with agricultural output. Given the relatively small scale of the operation, it is not likely that the workers of Baojia were professional smelters.
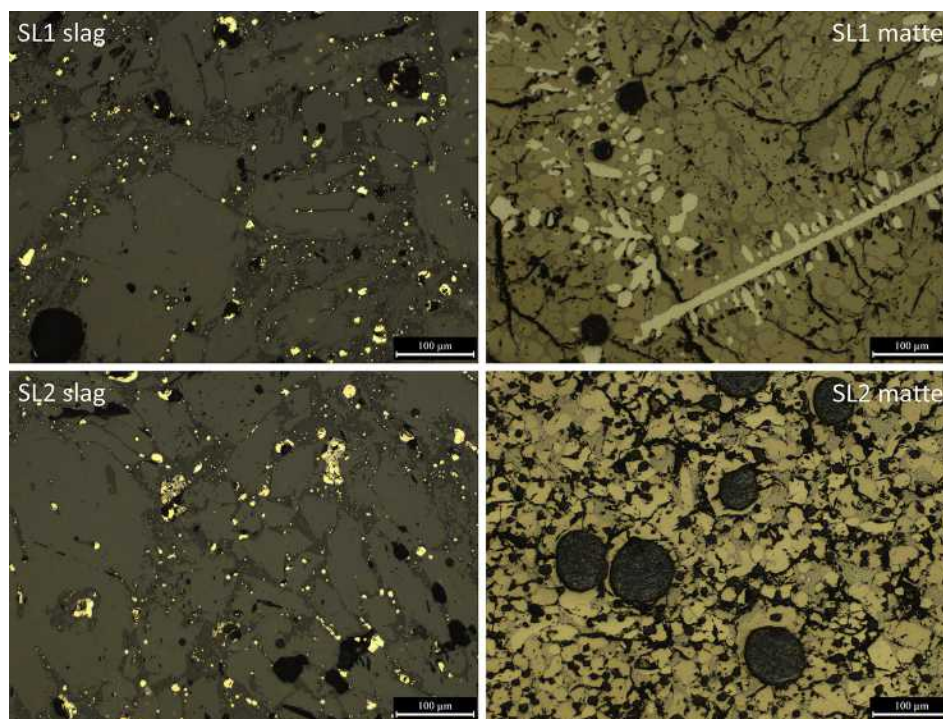

Fig. 17. Optical micrographs of SL1 and SL2 slag and matte. Slag consists of a glassy matrix with predominant fayalite and frequent matte prills. Matte cakes from both experiments are dominated by pyrrhotite. Dendritic metallic iron was also identified in SL1 matte.
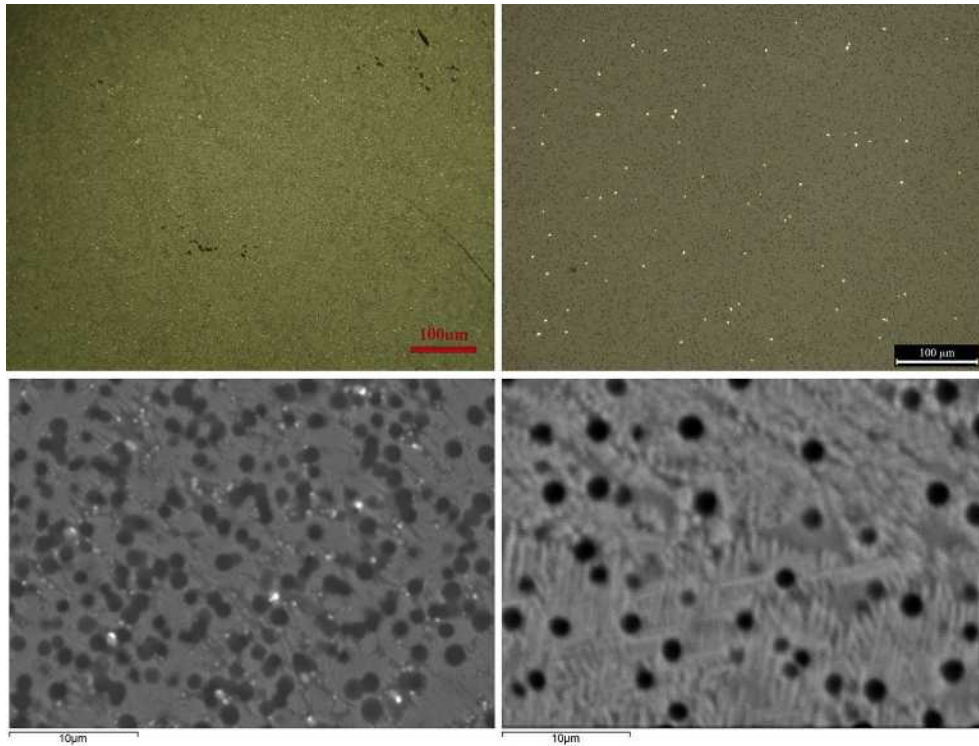
Fig. 18. Optical and high magnification BSE images of the archaeological Baojia slag BJG-slag-1-5 (left) and the experimental SL4 slag (right). Both cases have the same phase separation microstructure consisting of bright grey and globular dark phases, even though SL4 is based on an originally fayalitic slag.

Winning some silver and gold from ores in a relatively simple manner would be appealing for them, but importing lead from another county to squeeze out the last drops of silver might have been beyond their means of organisation and capital investment.

Fig. 19. FeO–Al$_2$O$_3$–SiO$_2$ ternary diagram (after Muan, 1957). The Baojia slag samples mostly plot in an area of high melting temperatures, while the bloomery slag used in the experiments plotted in the area between isotherms of 1150 and 1200 °C.

8. Conclusion and outlook

Production remains from the site of Baojia in Jiangxi province, central-south China provide us a unique insight into gold and silver production in the imperial period of China, barely studied by previous researchers. Combining analyses of archaeological remains and laboratory experiments, the Baojia technology was reconstructed as smelting a mixture of sulphidic and gossan ores in a relatively low temperature furnace to produce lead bullion containing gold and silver, with metallic iron identified as the main reductant. Ore efficiency at this site was not high since much silver was lost in smelting by-products such as matte and speiss. Setting these technological choices in the geological and social contexts of this site we argue that the precious metal production in Baojia was operated by part-time smelters whose primary concern was not ore efficiency. Instead, they operated a relatively low-key and low-scale smelting process adapted to their limited organisational and technological capacity.

It is beyond the scope of this paper to discuss the origin and spread of IRP in ancient times but it is certainly an interesting question to explore in the future. The current research for the first time demonstrated that this technology could be practiced by early smelters in a relatively simple manner. It also provides the reference data to search for evidence of this technology elsewhere, and it is hoped that more studies on this issue will help to answer where and how the nonprofessional workers such as those at the site of Baojia would have learned to smelt their ore by IRP — if they were at all aware that they used this particular technology. The near-surface iron oxide-rich gossan accessible to small-scale miners and smelters could just have made for a fortuitous self-fluxing charge combining residual lead-bearing primary sulphidic ore and auriferous quartz gangue, suitable for furnaces that did not
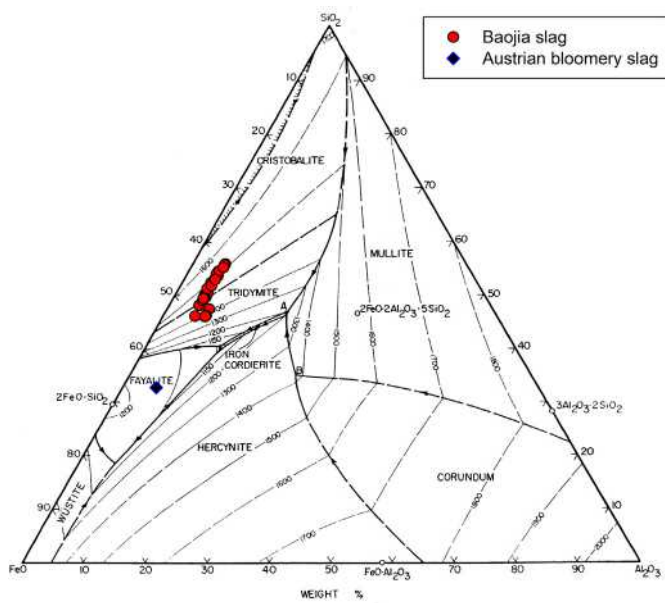
require the capital investment, level of organisation and economic network needed to operate the powerful blast furnaces of the time.

Finally, the ongoing research also gives new insights beyond the smelting mechanism of lead and precious metals. Sulphur is demonstrated to have a critical influence on the melting temperature and chemical behaviour of slag. In sulphur-rich systems, iron reduction can take place at relatively low temperature and mildly reducing conditions. More broadly, this research proved the importance of experimental simulation in interpreting a relatively unusual technology.

Acknowledgements

Appendix A. Supplementary data

Supplementary data related to this article can be found at http://dx.doi.org/10.1016/j.jas.2014.12.023.

References

Bachmann, H.G., 1982. The Identification of Slags from Archaeological Sites. Institute of Archaeology, London.

Bachmann, H.G., 1995. Sophisticated Roman recovery techniques for gold. Inst. Archaeo-Metall. Stud. Newsl. 19, 7—9.

Baker, D.R., Moretti, R., 2011. Modeling the solubility of sulfur in magmas: a 50-year old geochemical challenge. Rev. Mineral. Geochem. 73, 167—213.

Bayley, J., Crossley, D., Ponting, M., 2008. Metals and Metalworking: a Research Framework for Archaeometallurgy. The Historical Metallurgy Society, London.

Blanchard, I., 1992. Technical implications of the transition from silver to lead smelting in twelfth century England. In: Willies, L., Cranstone, D. (Eds.), Boles and Smeltmills. Historical Metallurgy Society, Matlock Bath, pp. 9—12.

Bunker, E.C., 1993. Gold in the ancient Chinese world: a cultural puzzle. Artibus Asiae 53, 27—50.

Bunker, E.C., 1994. The enigmatic role of silver in China. Orientations 25, 73—78.

Cohen, C.R., Rehren, Th, Buren, M.V., 2009. When the wind blows: environmental adaptability in current day silver production within the Bolivian Andes. In: Moreau, J.F., Auger, R., Chabot, J., Herzog, A. (Eds.), Proceedings of the 36th International Symposium on Archaeometry, CELAT, Université Laval Québec, pp. 465—475.

Craddock, P.T., 1995. Early Metal Mining and Production. Edinburgh University Press, Edinburgh.

Craddock, P.T., Freestone, I.C., Gale, N.H., Meeks, N.D., Rothenberg, B., Tite, M.S., 1985. The investigation of a small heap of silver smelting debris from Rio Tinto, Huelva, Spain. In: Craddock, P.T., Hughes, M.J. (Eds.), Furnaces and Smelting Technology in Antiquity. British Museum, London, pp. 199—217.

Dube, R.K., 2006. The extraction of lead from its ores by the iron-reduction process- a historical perspective. JOM 58, 18—23.

Erick, H.R., Ozok, H., 1994. High-temperature phase relations and thermodynamics in the iron-lead-sulfur system. Metall. Trans. B 25B, 53—61.

Fincham, C.J.B., Richardson, F.D., 1954. The behaviour of sulphur in silicate and aluminate melts. Proc. R. Soc. Lond. Ser. A 223, 40—62.

Fonseca, R.O.C., Campbell, I.H., O'Neill, H.S.C.O., Fitzgerald, J.D., 2008. Oxygen solubility and speciation in sulphide-rich mattes. Geochim. Cosmochim. Acta 72, 2619—2635.

Freestone, I.C., Craddock, P.T., Hegde, K.T.M., Hughes, M.J., Paliwal, H.V., 1985. Zinc production at Zawar, Rajasthan. In: Craddock, P.T., Hughes, M.J. (Eds.), Furnaces and Smelting Technology in Antiquity. British Museum, London, pp. 229—244.

Gill, M.C., 1992. An outline of the chemistry of lead smelting. In: Willies, L., Cranstone, D. (Eds.), Boles and Smeltmills. Historical Metallurgy Society, Matlock Bath, p. 3.

Golas, P.J., 1999. Science and Civilisation in China: Chemistry and Chemical Technology; Part XIII: Mining, vol. 5. Cambridge University Press, Cambridge.

Gyllensvard, B., 1957. T'ang Gold and Silver. In: Bulletin of the Museum of Far Eastern Antiquities 29.

Hauptmann, A., 2007. The Archaeometallurgy of Copper: Evidene from Faynan, Jordan. Springer-Verlag, Berlin Heidelberg.

Hauptmann, A., 2014. The investigation of archaeometallurgical slag. In: Roberts, B.W., Thornton, C.P. (Eds.), Archaeometallurgy in Global Perspective. Springer, New York, Heidelberg, Dordrecht, London, pp. 91—105.

Institute of Qing History, Department of Archive, RUC, 1983. Mining Industry of the Qing Dynasty (清代的矿业). Zhonghua Book Company, Beijing (in Chinese).

Kaiura, G.H., Toguri, J.M., 1979. Natural convective mass transfer rates between solid magnetite and molten mattes. Metall. Trans. B 10, 595—606.

Kassianidou, V., 1992. Monte Romero (Huelva), a Silver Production Workshop of the Tartessian Period in SW Spain. Institute of Archaeology, University College London, London.

Kassianidou, V., 1993. The production of silver in Monte Romero, a 7th century B.C. workshop in Huelva, Spain. Pap. Inst. Archaeol. 4, 37—47.

Kassianidou, V., 1998. Was silver actually recovered from speiss in antiquity? In: Rehren, Th, Hauptmann, A., Muhly, J.D. (Eds.), Metallurgica Antiqua, Der Anschnitt, Beiheft 8. Deutsches Bergbau-Museum, Bochum, pp. 69—76.

Katō, S., 2006. Study of Gold and Silver in Tang and Song: Based on the Currency Function of Gold and Silver (唐宋金银之研究—以金银之货币机能为中心). Translated from Japanese version published in 1926 by Zhonghua Book Company. Zhonhua Book Company, Beijing (in Chinese).

Killick, D., Gordon, R.B., 1989. The mechanism of iron production in the bloomery furnace. In: Farquhar, R.M., Hancock, R.G.V., Pavlish, L.A. (Eds.), Proceedings of the 26th International Archaeometry Symposium, Toronto, pp. 120—123.

Maclean, W.H., 1969. Liquidus phase relations in the FeS-FeO-Fe$_3$O$_4$-SiO$_2$ system, and their application in geology. Econ. Geol. 64, 865—884.

Marechal, J.R., 1985. Methods of ore roasting and the furnaces used. In: Craddock, P.T., Hughes, M.J. (Eds.), Furnaces and Smelting Technology in Antiquity. British Muesum, London, pp. 29—41.

Muan, A., 1957. Phase equilibria at liquidus temperatures in the system iron oxide-Al$_2$O$_3$-SiO$_2$ in air atmosphere. J. Am. Ceram. Soc. 40, 121—133.

Percy, J., 1870. The Metallurgy of Lead. John Murray, London.

Poulson, S.R., Ohmoto, H., 1990. An evaluation of the solubility of sulfide sulfur in silicate melts from experimental data and natural samples. Chem. Geol. 85, 57—75.

Qi, D., 1999. Research on Tang Gold and Silver (唐代金银器研究). Chinese Academy of Social Science Publication, Beijing (in Chinese).

Rehder, J.E., 1994. Blowpipes versus bellows in ancient metallurgy. J. Field Archaeol. 21, 345—350.

Rehren, Th, Prange, M., 1998. Lead metal and patina: a comparison. In: Rehren, Th, Hauptmann, A., Muhly, J.D. (Eds.), Metallurgica Antiqua: in Honour of Hans-Gert Bachmann and Robert Maddin. (= Der Anschnitt, Beiheft 8). Deutsches Bergbau-Museum, Bochum, pp. 183—196.

Rehren, Th, Boscher, L., Pernicka, E., 2012. Large scale smelting of speiss and arsenical copper at Early Bronze Age Arisman. North-West Iran J. Archaeol. Sci. 39, 1717.

Rehren, Th, Charlton, M., Chirikure, S., Humphris, J., Ige, A., Veldhuijzen, H.A., 2007. Decisions set in slag: the human factor in African iron smelting. In: La Niece, S., Hook, D., Craddock, P.T. (Eds.), Metals and Mines: Studies in Archaeometallurgy. Archetype Books, London, pp. 211—218.

Rosenqvist, T., 1983. Principles of Extractive Metallurgy. McGraw-Hill Book Company, New York.

Sharma, R.C., Chang, Y.A., 1979. Thermodynamics and phase relationships of transition metal-sulfur systems: Part III. Thermodynamic properties of the Fe-S liquid phase and the calculation of the Fe-S phase diagram. Metall. Trans. B 10, 103—108.

Shennan, S., 1999. Cost, benefit and value in the organization of early European copper production. Antiquity 73, 353—363.

Starykh, R.V., Sineva, S.I., Zakhryapin, S.B., 2010. Study of the liquidus and solidus surfaces in the quaternary Fe-Ni-Cu-S system: IV. Costruction of a meltability diagram and determination of miscibility gap boundaries for the ternary Cu-Fe-S sulfide system. Russ. Metall. 11, 1025—1031.

Tholander, E., 1989. Microstructure examination of slags as an instrument for identification of ancient iron-making processes. In: Pleiner, R. (Ed.), Archaeometallurgy of Iron Results Achieved 1967-1987: Symposium Liblice 1987, Prague, pp. 35—42.

Thornton, C.P., Rehren, Th, Pigott, V.C., 2009. The production of speiss (iron arsenide) during the Early Bronze Age in Iran. J. Archaeol. Sci. 36, 308—316.

Tylecote, R.F., 1987. The Early History of Metallurgy in Europe. Longman, London & New York.

Tylecote, R.F., Merkel, J.F., 1985. Experimental smelting techniques: achievements and Future. In: Craddock, P.T., Hughes, M.J. (Eds.), Furnaces and Smelting Technology in Antiquity. British Museum Occasional Paper 48, London, pp. 3–20.

Voisin, L., Itagaki, K., 2006. Phase relations, activities and minor element distribution in Cu-Fe-S and Cu-Fe-S-As systems saturated with carbon at 1473 K. Mater. Trans. 47, 2963–2971.

Wang, L., 2005. The Study of Mining and Metal Production Industry in the Song Dynasty (宋代矿冶业研究). Hebei University Press Baoding, Hebei (in Chinese).

Xie, P., Rehren, Th, 2009. Scientific analysis of lead-silver smelting slag from two sites in China. In: Rehren, Th, Mei, J. (Eds.), Metallurgy and Civilisation: Eurasia and beyond, Archetype in Association with the University of Science and Technology Beijing and the Institute for Archaeo-metallurgical Studies, London, London, pp. 177–183.

Yazawa, A., 1956. Fundamental studies on copper smelting V: mutual dissolution between matte and slag produced in system Cu_2S-FeS-FeO-SiO_2. J. Min. Inst. Jpn. 72, 305–311.

Yazawa, A., Kameda, M., 1953. Fundamental Studies on Copper Smelting I: Partial Liquidus Diagram for FeS-FeO-SiO_2 System. Technical Reports of Tohoku University 18, pp. 40–58.

Yi, B., 1972. Preliminary study of silver production technology in the Tang period (唐代冶银术初探). Cult. Relics 6, 40–43 (in Chinese).

Zhang, H., 1954. A Record of Ancient Mines (古矿录). Geology Press, Beijing (in Chinese).

Zhou, W., Liu, S., Liu, H., Chen, J., 2014. A preliminary study of traditional Chinese crucible lead smelting technology (中国传统坩埚炼铅技术初探). Stud. Hist. Nat. Sci. 33, 201–215 (in Chinese).